



Research article

Identification of potential key ferroptosis- and autophagy-related genes in myelomeningocele through bioinformatics analysis

Xiuwei Wang^a, Kaixin Wei^b, Min Wang^{c,**}, Li Zhang^{b,d,*}

^a Beijing Municipal Key Laboratory of Child Development and Nutriomics, Translational Medicine Laboratory, Capital Institute of Pediatrics, Beijing, 100020, China

^b Department of Biochemistry and Molecular Biology, Shanxi Medical University, Taiyuan, 030001, Shanxi, China

^c Department of Physiology, College of Medicine, Jiaying University, Jiaying, 314001, Zhejiang, China

^d Department of Hepatobiliary and Pancreatic Surgery and Liver Transplant Center, The First Hospital of Shanxi Medical University, Taiyuan, 030001, Shanxi, China

ARTICLE INFO

Keywords:

Myelomeningocele
Ferroptosis
Autophagy
Gene expression omnibus
Enrichment analysis
Bioinformatics

ABSTRACT

Myelomeningocele is a common congenital anomaly associated with polygenic disorders worldwide. However, the intricate molecular mechanisms underlying myelomeningocele remain elusive. To investigate whether ferroptosis and ferritinophagy contribute to the pathomechanism of myelomeningocele, differentially expressed genes (DEGs) were identified as novel biomarker and potential treatment agents. The GSE101141 dataset from Gene Expression Omnibus (GEO) was analyzed using GEO2R web tool to obtain DEGs based on $|\log_2$ fold change (FC)| ≥ 1.5 and $p < 0.05$. Two datasets from the Ferroptosis Database (481 genes) and Autophagy Database (551 genes) were intersected with the DEGs from the GSE101141 dataset to identify ferroptosis- and autophagy-related DEGs using Venn diagrams. Functional and pathway enrichment, protein-protein interaction (PPI) network analyses were performed, and candidate genes were selected. Transcription factors (TFs), microRNAs (miRNAs), diseases and chemicals interacting with the candidate genes were identified. Receiver operating characteristic (ROC) curve analysis was performed to validate the diagnostic value of the candidate genes. Sixty ferroptosis-related and 74 autophagy-related DEGs were identified. These DEGs are involved in FoxO signaling pathway. Six candidate genes (*EGFR*, *KRAS*, *IL1B*, *SIRT1*, *ATM*, and *MAPK8*) were selected. miRNAs such as hsa-miR-27a-3p, hsa-miR-877-5p, and hsa-miR-892b, and TFs including P53, POU3F2, TATA are involved in regulation of candidate genes. Diseases such as schizophrenia, fibrosis, and neoplasms are the most relevant to the candidate genes. Chemicals, such as resveratrol, curcumin, and quercetin may have significant implications in the treatment of myelomeningocele. The candidate genes, especially *MAPK8*, also showed a high diagnostic value for myelomeningocele. These results help to shed light on the molecular mechanism of myelomeningocele and may provide new insights into diagnostic biomarker in the amniotic fluid and potential therapeutic agents of myelomeningocele.

* Corresponding author. Department of Hepatobiliary and Pancreatic Surgery and Liver Transplant Center, The First Hospital of Shanxi Medical University, Taiyuan, 030001, Shanxi, China

** Corresponding author. Department of Physiology, College of Medicine, Jiaying University, Jiaying, Zhejiang, 314001, China.

E-mail addresses: wangmin3826@zjxu.edu.cn (M. Wang), zhangli3788@163.com (L. Zhang).

<https://doi.org/10.1016/j.heliyon.2024.e29654>

Received 8 October 2023; Received in revised form 10 April 2024; Accepted 11 April 2024

Available online 16 April 2024

2405-8440/© 2024 The Author(s). Published by Elsevier Ltd. This is an open access article under the CC BY-NC license (<http://creativecommons.org/licenses/by-nc/4.0/>).

1. Introduction

Myelomeningocele, also known as open spina bifida, is a phenotype of neural tube defects (NTDs) that occurs because of incomplete closure of the spinal neural tube during embryonic development and leads to physical disabilities [1,2]. This causes physical and psychological trauma to children and increase the financial burden on the family. Although myelomeningocele is a common birth defect, its etiology remains unclear. Growing evidence from genomic approaches and candidate gene studies have suggested that gene variants are involved in different molecular pathways that increase genetic susceptibility to myelomeningoceles. Ortiz-Cruz et al. [3] conducted a multicenter population-based survey of 16 telethon centers of 16 Mexican in 500 family trios and revealed an association of gene variants in the hedgehog, Wnt, planar cell polarity, and cilia pathways with myelomeningocele occurrence location. Hebert et al. [4] demonstrated that 17 genes with rare deleterious variants in the Wnt signaling pathway were associated with an increased risk of myelomeningocele, as shown through the mutational burden analysis of exome sequencing data from 511 patients with myelomeningocele. These data suggest that myelomeningocele is a complex disease with multiple gene interactions and that the Wnt signaling pathway plays a crucial role. Previous studies have shown that the Wnt signaling pathway regulates ferroptosis and is also involved in autophagy. Therefore, in the present study, we investigated whether ferroptosis and autophagy contribute to the etiology of myelomeningoceles.

Ferroptosis, a cell death pathway associated with intracellular phospholipid peroxidation, is regulated by multiple metabolic reactions, including redox homeostasis, iron homeostasis, mitochondrial activity, amino acid metabolism, and numerous signaling pathways [5]. Although limited literature exists on the relationship between ferroptosis and myelomeningoceles, growing evidence suggests that ferroptosis is associated with neural development. Qi et al. reported that the ferroptosis inducer, erastin, significantly decreased the axonal length of motor nerves in zebrafish embryos, and ferrostatin reversed the impaired motor neuron development, suggesting that activated ferroptosis could impair neurogenesis [6]. Glutathione peroxidase 4 (GPX4) is the key regulator that could inhibit the progress of ferroptosis [7]. Transferrin receptor 1 (TfR1) mediates cellular iron uptake and promote ferroptosis [8]. Maternal sevoflurane exposure decreases GPX4 levels, increases TfR1 expression, and impairs neurogenesis in the embryonic prefrontal cortex, indicating that ferroptosis is involved in neurotoxicity [9]. These data suggest that ferroptosis is closely associated with neural development.

Autophagy is an intracellular process that removes unwanted cellular components and is closely associated with NTDs. The autophagy regulator gene *AMBRA1* mutation or functional deficiency contributed to the etiology of NTDs [10,11]. Maternal diabetes suppresses autophagy in the neuroepithelium of mice, leading to NTD formation [12]. Ferritinophagy is a form of autophagy that is specifically related to ferritin [13,14]. Nuclear receptor coactivator 4 (NCOA4) functions as a selective autophagy receptor that binds to ferritin, promoting ferritinophagy and releasing iron from ferritin to enhance the sensitivity of ferroptosis [15]. Sun et al. [16] observed ferritinophagy in fetal growth restriction placentas and silencing of NCOA4 ameliorated ferroptosis in trophoblast, indicating that autophagy mediates ferroptosis and is involved in embryonic development. P53, as a candidate gene for NTDs, mediates transcriptional repression of solute carrier family 7 member 11 (SLC7A11), which is critical for ferroptosis in embryonic development [17]. Therefore, these studies indicate that autophagy may be involved in ferroptosis, contributing to the development of NTDs.

Although ferroptosis contributes to neural and embryonic development, few studies have investigated the potential relationship between ferroptosis-related genes and NTD pathogenesis. Insufficient data available through searches and restricted analytical strategies have limited evidence supporting the role of ferroptosis-related genes in myelomeningoceles. In the present study, data mining and analytical techniques were used to screen for DEGs between patients with myelomeningocele and controls. Venn diagrams were used to obtain overlapping ferroptosis- and autophagy-related DEGs, and functional enrichment analyses were performed. PPI networks were used to identify hub genes, which may be potential ferroptosis- and autophagy-related biomarkers for the pathogenesis of myelomeningocele. TFs, miRNAs, diseases, and chemicals that interact with candidate genes were performed using networkanalyst and visualized using cytoscape v3.8.2 software. ROC analysis was performed to validate the diagnostic value of candidate genes. The aim of this study was to determine the pivotal ferroptosis-related molecular features involved in the pathogenesis of myelomeningocele using an integrated bioinformatics methodology, to provide novel perspectives on the molecular mechanisms underlying the occurrence of myelomeningocele, and to suggest a novel diagnostic biomarker in the amniotic fluid and a potential therapeutic agent for myelomeningocele.

2. Materials and methods

2.1. GEO dataset

The keywords "Neural tube defects," "*Homo sapiens*," and "Amniotic fluid," were used to search the expression datasets from GEO (<https://www.ncbi.nlm.nih.gov/geo/>). The dataset GSE101141 stored by Tarui et al. [18] was downloaded from GEO. This dataset included ten amniotic fluid supernatants from pregnant women with open myelomeningoceles and ten amniotic fluid supernatants from sex- and gestational age-matched fetuses without myelomeningoceles as controls, based on the Human Genome U133 Plus 2.0 arrays. A dataset of 20 samples was obtained from public databases; hence, patient informed consent and approval from ethics committee were unnecessary.

2.2. DEGs identification

The online analysis tool-GEO2R was used to identify DEGs [19]. The screening criteria was set as $|\log_2 \text{fold change (FC)}| \geq 1.5$ and p

< 0.05 for the differential gene expression analysis. Two datasets were obtained from the Ferroptosis Database (481 genes, <http://www.zhounan.org>) and Autophagy Database (551 genes, <http://hamdb.scbdd.com>) [20] and intersected with the DEGs from GSE101141 to identify ferroptosis- and autophagy-related DEGs, respectively. Venn diagrams of DEGs were generated using the online tool Venny2.1, and a heat map of DEGs was generated using the online tool NetworkAnalyst 3.0 (<https://www.networkanalyst.ca>) [21].

2.3. Functional enrichment analysis

Functional enrichment analyses of the DEGs were performed using DAVID (<https://david.ncicrf.gov>) [22], SRplot (<https://www.bioinformatics.com.cn>), Webgestalt (<https://www.webgestalt.org>) [23], and Metascape (<https://metascape.org>) [24]. We uploaded the ferroptosis- and autophagy-related DEGs to DAVID, SRplot, and the gene set enrichment analysis (GSEA) of WebGestalt for further study and obtained the results of Gene Ontology (GO) and Kyoto Encyclopedia of Genes and Genes (KEGG) analyses. The ferroptosis- and autophagy-related DEGs were uploaded to Metascape for gene function annotation.

2.4. Protein-protein interaction network analysis

The ferroptosis- and autophagy-related DEGs were uploaded to the online database-STRING (<https://cn.string-db.org>) [25] to explore the PPIs with the following settings: full STRING network for network type, evidence for meaning of network edges, and medium confidence (0.400) for minimum required interaction score. Cytoscape [26,27] v3.8.2 software was used to visualize the PPI network with combined score>0.4. Hub genes were obtained from the PPI network.

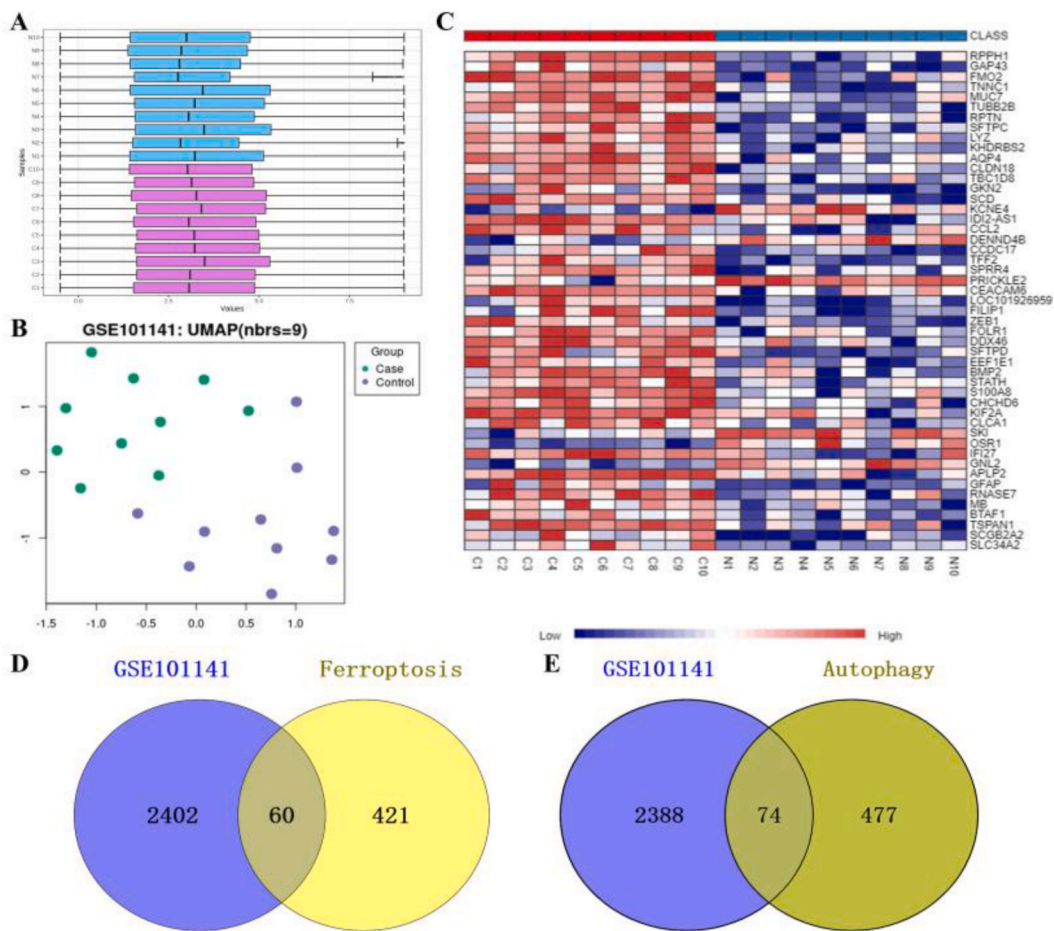


Fig. 1. Identification of DEGs in the GSE101141 GEO dataset. A Normalization of the GSE101141 dataset was performed using Log2 transformation: N, Control; C, myelomeningocele; B UMAP plot; C Heat map of the dataset demonstrated distinguished features between myelomeningocele and control samples; D and E Venn diagram of GSE101141 and ferroptosis- and autophagy-related genes.

2.5. Gene-miRNA, TF-genes, interactions, and TF-miRNA coregulatory network of candidate genes

Candidate genes were obtained from the intersection of two datasets of ferroptosis- and autophagy-related DEGs. The miRWalk database (<http://mirwalk.umm.uni-heidelberg.de>) was used to establish the gene-miRNA interaction network to predict the relationship between the candidate genes and miRNA [28]. The JASPAR database (<https://jaspar.genereg.net>) was used to obtain the TF-gene interaction network [29]. Furthermore, the RegNetwork database (<https://regnetworkweb.org>) was used to construct a TF-miRNA coregulatory network [30]. These networks were constructed using NetworkAnalyst and visualized using Cytoscape v3.8.2 software.

2.6. Gene-disease associations

The DisGeNET database (<https://www.disgenet.org>) [31] was used to analyze the association between diseases and candidate genes using the NetworkAnalyst platform.

2.7. Protein-chemical interactions

The Comparative Toxicogenomics Database (CTD, <https://ctdbase.org>) [32] was used to investigate the relationship between candidate genes and chemicals using the NetworkAnalyst platform. ChemSpider (<http://www.chemspider.com>) was used to identify the chemical structure.

2.8. Candidate genes diagnosis model construction

ROC curves of the candidate genes were constructed using the Xiantao website (<https://www.xiantaozi.com>).

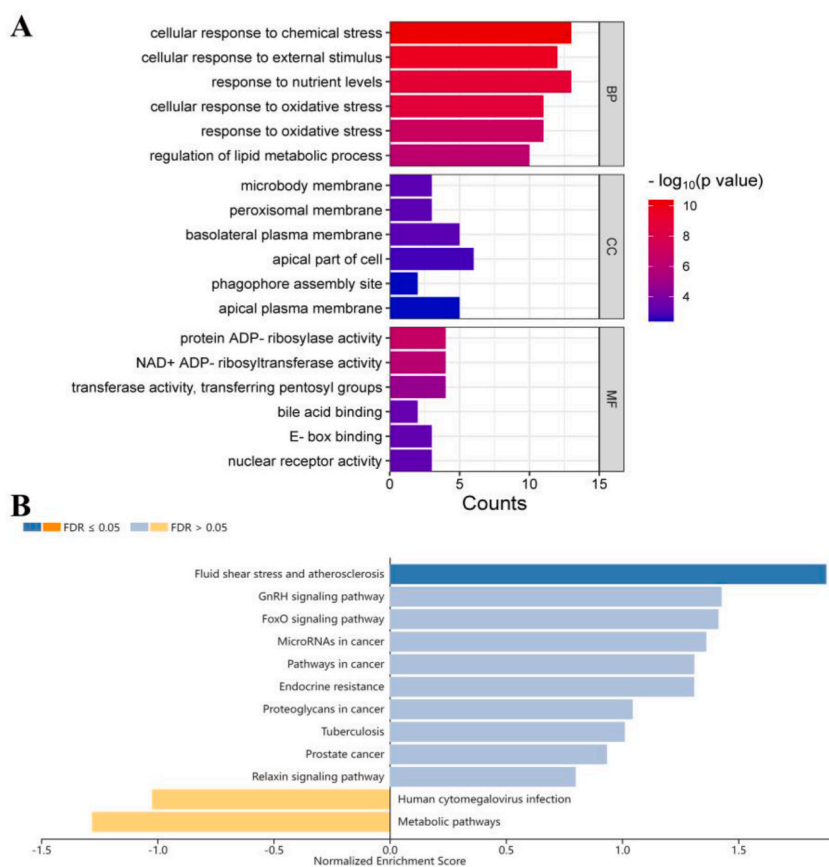


Fig. 2. Functional enrichment analysis of ferroptosis-related DEGs. A GO enrichment analysis of ferroptosis-related DEGs using SRplot: BP, biological process; CC, cellular component; MF, molecular function; B KEGG pathway enrichment analysis of ferroptosis-related DEGs using WebGestalt.

3. Results

3.1. Identification of DGEs in GSE101141

The expression profiling dataset GSE101141 was downloaded from the GEO database. The distribution of values of the selected samples in GSE101141 was suitable for differential expression analysis after log transformation and normalization (Fig. 1A). Uniform Manifold Approximation and Projection (UMAP) showed clusters among the sample groups (Fig. 1B). The DEGs (2462 genes) were obtained from comparing the open myelomeningocele and control with $p < 0.05$ and $|\log_2(\text{Fold Change})| \geq 1.5$. There were 752 downregulated and 1710 upregulated genes in the GSE101141 dataset. A heat-map of the DEGs is shown in Fig. 1C. Two datasets were obtained, including 481 genes from the Ferroptosis Database (FerrDb) and 551 genes from the Autophagy Database (HAMdb), and intersected with the DEGs from GSE101141 to identify ferroptosis- and autophagy-related DEGs, respectively. Sixty ferroptosis-related and seventy-four autophagy-related DEGs were identified using a Venn diagram (Fig. 1D and E).

3.2. Enrichment analysis of ferroptosis-related DEGs

Sixty ferroptosis DEGs (45 upregulated and 15 downregulated; Supplementary Table S1) were classified as ferroptosis drivers, suppressors, and markers according to the FerrDb database (Supplementary Table S2). Analysis of ferroptosis-related DEGs for the enrichment pathway was performed using SRplot, WebGestalt and Metascape. GO analysis categories included biological processes, cellular components, and molecular functions. The enriched biological process categories included cellular response to chemical stress, cellular response to external stimulus, response to nutrient levels, and oxidative stress. The primary enriched cellular component categories included microbody membrane, peroxisomal membrane, basolateral plasma membrane, and apical part of cell. The primary enriched molecular function categories included ADP-ribosylase, NAD + ADP-ribosyltransferase, and transferase activities (Fig. 2A). The results of KEGG enrichment analysis showed that the ferroptosis-related DEGs were primarily enriched in metabolic pathways, fluid shear stress and atherosclerosis, the GnRH signaling pathway, and the FoxO signaling pathway (Fig. 2B). The DEGs were uploaded to Metascape, and the results showed that biological processes were enriched in the response to nutrient levels, cellular response to chemical stress, and cellular response to lipid (Supplementary Fig. S1).

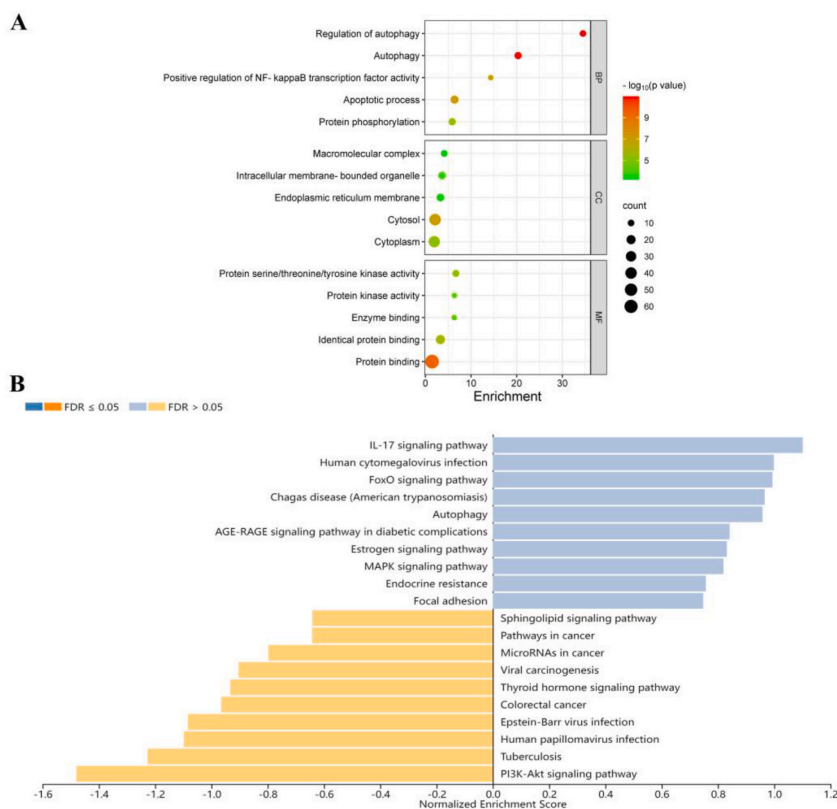


Fig. 3. Functional enrichment analysis of autophagy-related DEGs. A GO enrichment analysis of autophagy-related DEGs using DAVID and SRplot: BP, biological process; CC, cellular component; MF, molecular function; B KEGG pathway enrichment analysis of autophagy-related DEGs using WebGestalt.

3.3. Enrichment analysis of autophagy-related DEGs

Seventy-four DEGs related to autophagy (50 upregulated and 24 downregulated; [Supplementary Table S2](#)) were uploaded into DAVID, SRplot, WebGestalt and Metascape. The GO analysis results showed that the genes were markedly enriched in the regulation of autophagy, apoptotic processes of biological processes, micromolecular complexes, cytosol, and cytoplasm of cellular components, protein serine/threonine/tyrosine kinase activity, identical protein binding, and protein binding with regard to molecular function ([Fig. 3A](#)). KEGG analysis showed that these genes were significantly enriched in the PI3K-Akt signaling pathway, IL-17 signaling pathway, FoxO signaling pathway, and autophagy ([Fig. 3B](#)). The 74 genes uploaded to Metascape showed that the biological processes were significantly enriched in the regulation of autophagy and positive regulation of cell death ([Supplementary Fig. S2](#)).

3.4. PPI network analysis

The PPI networks of ferroptosis- and autophagy-related DEGs were constructed using STRING and Cytoscape v3.8.2. Network nodes represent proteins. The edges represent protein-protein associations. The blue nodes represent downregulated genes and the orange nodes represent upregulated genes ([Fig. 4A and B](#)). The top ten hub genes of ferroptosis- and autophagy-related DEGs were identified using Cytoscape v3.8.2 (MCC, [Fig. 4C and D](#)). Six candidate genes (*EGFR*, *KRAS*, *IL1B*, *SIRT1*, *ATM*, and *MAPK8*) were selected from the ferroptosis- and autophagy-related hub genes ([Fig. 4E](#)). The expression of *EGFR* was lower, and the levels of *KRAS*, *IL1B*, *SIRT1*, *ATM* and *MAPK8* were higher in the myelomeningocele group than in the control ([Fig. 5A](#)). GO and KEGG analyses showed that the candidate genes were enriched in the positive regulation of protein phosphorylation and gene expression of biological processes, cytosol and cytoplasm of cellular components, enzyme binding and adenosine triphosphate (ATP) binding of molecular function and FoxO signaling pathway of KEGG ([Fig. 5B–D](#)).

3.5. Candidate gene-miRNA interaction

Gene-miRNA analysis was performed on six candidate genes (*EGFR*, *KRAS*, *IL1B*, *SIRT1*, *ATM*, and *MAPK8*) using the miRWalk database. The gene-miRNAs interactions network was constructed based on the following criteria: score >0.90 and 3' untranslated region (UTR) as the target gene binding regions, then visualized using Cytoscape v3.8.2 ([Fig. 6A](#)). The results showed that hsa-miR-27a-3p, hsa-miR-877-5p, hsa-miR-892b, hsa-miR-155-5p, hsa-miR-92a-3p, and hsa-miR-18a-3p interacted most strongly with the

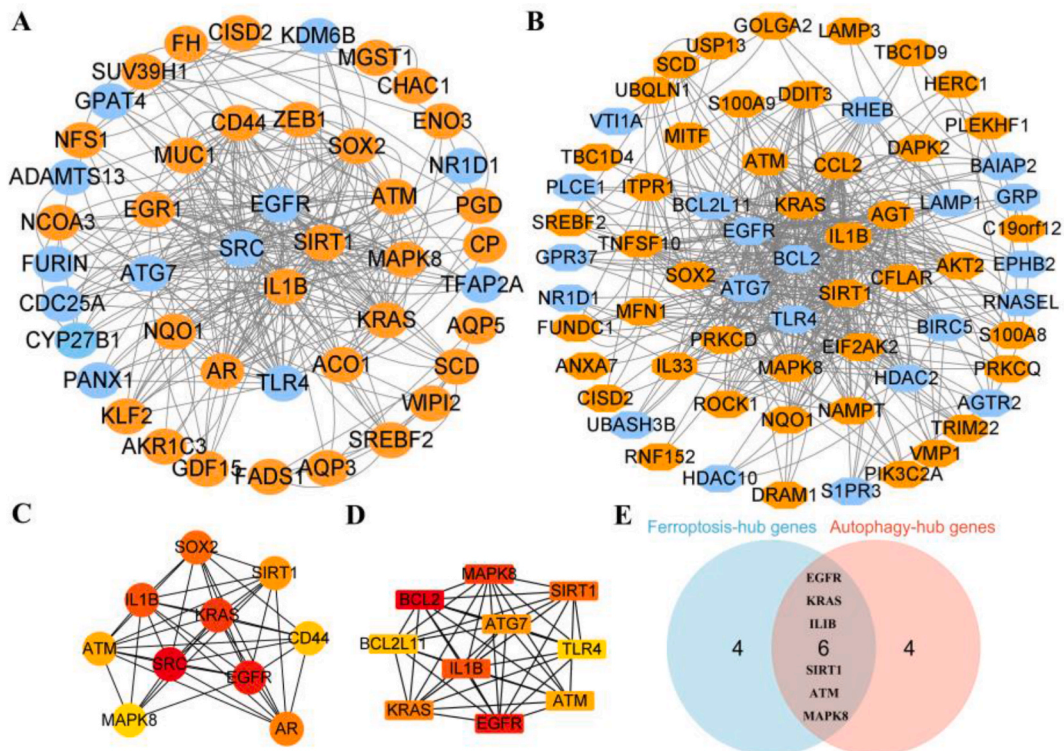


Fig. 4. PPI analysis of ferroptosis- and autophagy-related DEGs. A and B PPI analysis of ferroptosis- and autophagy-related DEGs: orange, upregulated genes; blue, downregulated genes; C and D Top ten hub genes of ferroptosis- and autophagy-related DEGs using MCC; E Candidate genes were selected from ferroptosis- and autophagy-related hub genes.

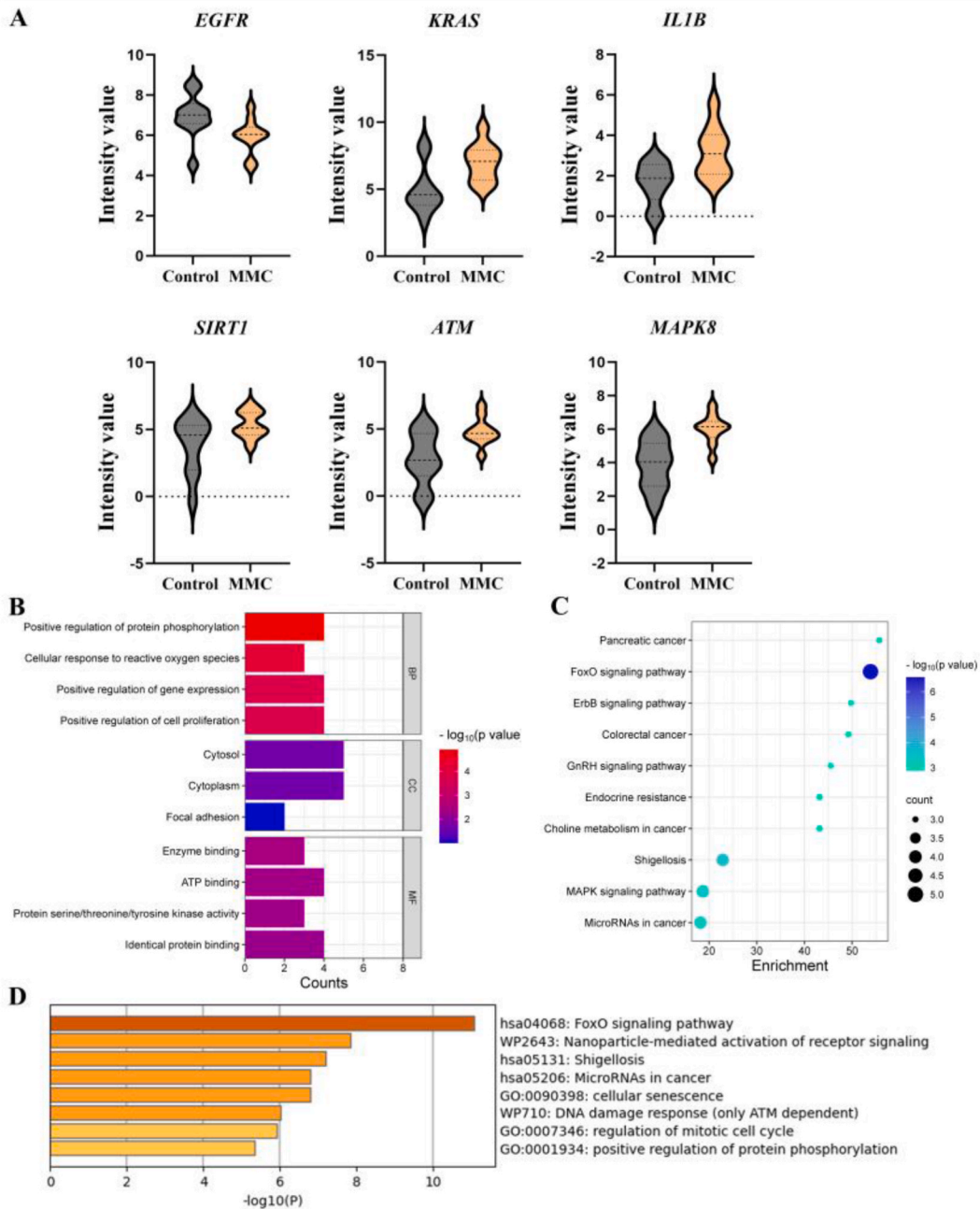


Fig. 5. Expression and function enrichment of candidate genes. A Expression of candidate genes from GSE101141; B and C GO and KEGG enrichment analyses of candidate genes using DAVID and SRplot: BP, biological process; CC, cellular component; MF, molecular function; D Enrichment term analysis of candidate genes using Meascape.

candidate genes.

3.6. Candidate gene-TF interactions

To investigate the potential modulatory relationships of the six candidate genes, the JASPAR database was used to predict TFs targeting the candidate genes, and visualized using Cytoscape v3.8.2, which included 19 nodes and 68 edges (Fig. 6B). TFs such as P53, POU3F2, TATA and E4BP4 have the potential to be novel diagnostic markers and therapeutic targets for myelomeningocele.

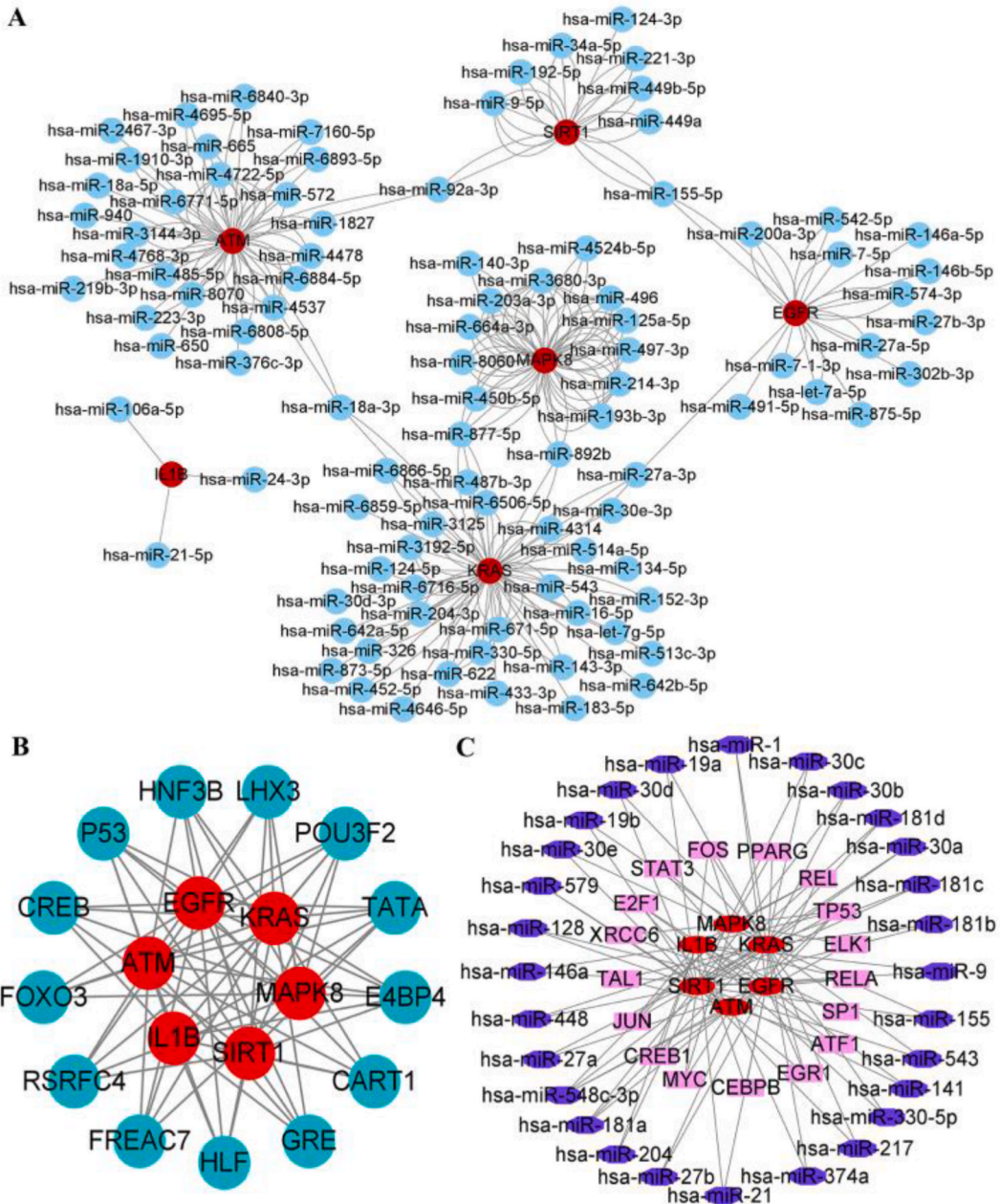


Fig. 6. Interaction network among miRNAs, TFs, and candidate genes. A Interaction network between candidate genes and targeted miRNAs: red, candidate genes; blue, miRNA; B Interaction network of TF-gene: red, gene; blue, TFs; C TF-miRNA coregulatory network of candidate genes: red, gene; pink, TFs; dark blue, miRNAs.

3.7. TF-miRNA co-regulatory network of candidate genes

To further explore the interplay between TFs, miRNAs and candidate genes, the reNetwork database was used to establish the TF-miRNA co-regulation network, which was visualized using Cytoscape v3.8.2 and contained 51 nodes and 103 edges (Fig. 6C). TFs such as TP53, E2F1, JUN, FOS, and MYC cooperate with miRNAs, including hsa-miR-548c-3p, hsa-miR-181a, hsa-miR-27b, hsa-miR-27a, and hsa-miR-1, to regulate candidate genes (*EGFR*, *KRAS*, *IL1B*, *SIRT1*, *ATM*, and *MAPK8*).

3.8. Gene-disease and protein-chemical interactions

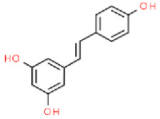
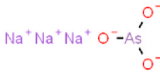
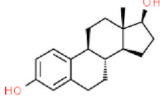
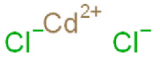
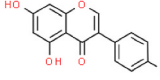
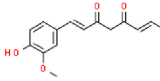
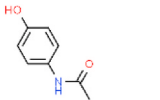
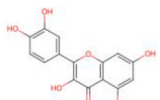
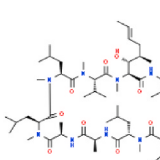
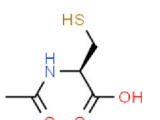
Gene-disease association and protein-chemical interactions were performed using the DisGeNET and CTD databases and visualized

using Cytoscape v3.8.2 (Figure 7A and B). The gene-disease network showed the most relevant genetic disorders, such as schizophrenia, fibrosis, mammary neoplasms, stomach neoplasms, and prostatic neoplasms. The protein-chemical network showed numerous interactions between the chemicals and candidate genes. The top ten chemicals that interacted with the candidate genes are summarized in Table 1.

3.9. Diagnosis model construction

ROC curve analysis was performed to validate the diagnostic value of candidate genes. The area under ROC curve (AUC) of *EGFR*, *KRAS*, *IL1B*, *SIRT1*, *ATM*, and *MAPK8* were 0.790, 0.810, 0.820, 0.720, 0.800, and 0.930, respectively. The six candidate genes, especially *MAPK8*, have high diagnostic value (Fig. 7C).

Table 1
Top 10 chemicals for hub genes.

ID	Chemicals	Chemical formula	Structure
D000077185	Resveratrol	$C_{14}H_{12}O_3$	
C017947	Sodium arsenite	$AsNa_3O_3$	
D004958	Estradiol	$C_{18}H_{24}O_2$	
D019256	Cadmium Chloride	$CdCl_2$	
D019833	Genistein	$C_{15}H_{10}O_5$	
D003474	Curcumin	$C_{21}H_{20}O_6$	
D000082	Acetaminophen	$C_8H_9NO_2$	
D011794	Quercetin	$C_{15}H_{10}O_7$	
D016572	Cyclosporine	$C_{62}H_{111}N_{11}O_{12}$	
D000111	Acetylcysteine	$C_5H_9NO_3S$	

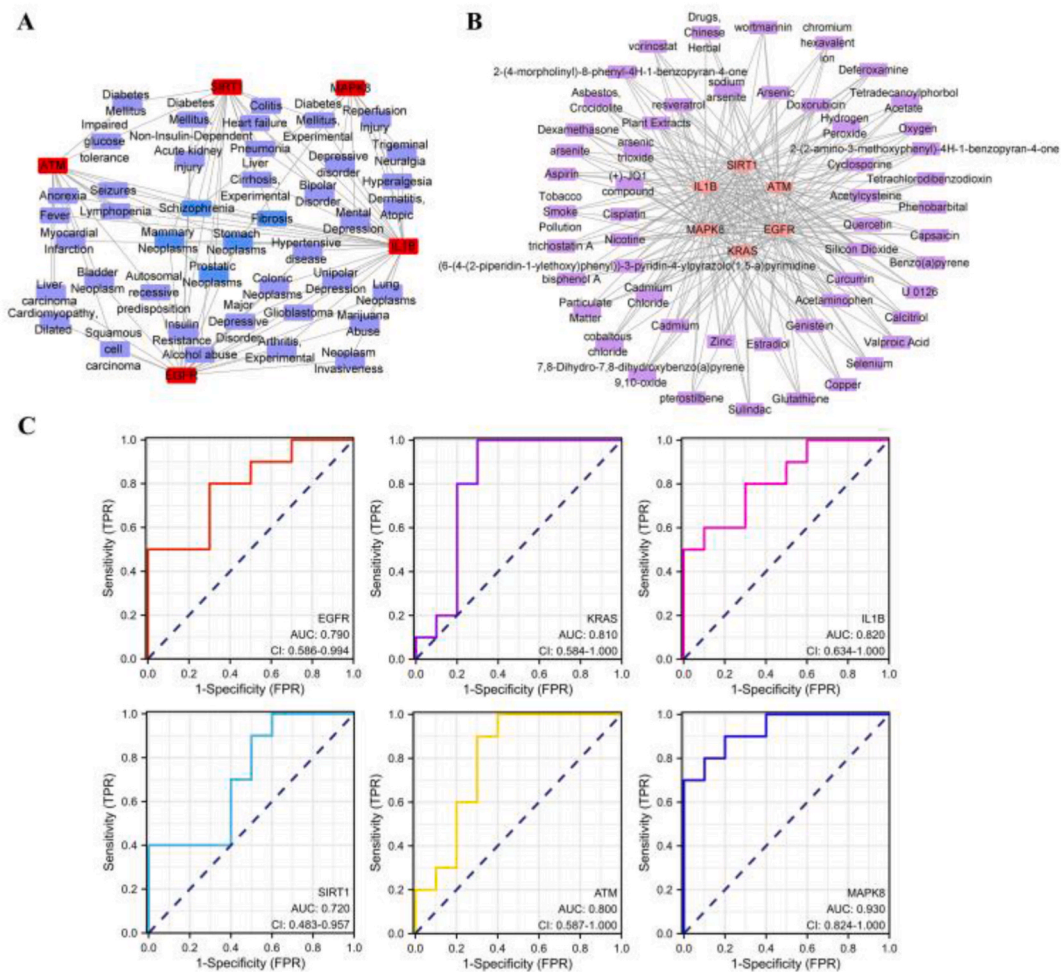


Fig. 7. Gene-disease associations and protein-chemical interactions. A Gene-disease association network: red, gene; light blue, disease; B Protein-chemical interaction network: pink, genes; pale purple: chemicals; C Analysis of the disease predictive abilities of the candidate genes.

4. Discussion

Myelomeningocele is characterized by failure of closure of the lumbosacral spinal neural tube during embryonic development and is a common NTD [1,2,33]. Genetic factors for the etiology of NTDs are estimated at 60–70 %, but the causative genes are still not fully understood. Therefore, exploring the pathogenesis of myelomeningoceles at the molecular level is required for the prevention, diagnosis, and treatment of NTDs, particularly myelomeningoceles. In this study, candidate genes and the underlying mechanisms of myelomeningocles were investigated using bioinformatic analysis. Sixty (45 upregulated and 15 downregulated) ferroptosis-related and 74 (50 upregulated and 24 downregulated) autophagy-related DEGs were identified from 20 samples in GSE101141. Further functional and pathway enrichment analyses showed that ferroptosis-related DEGs were involved in the response to chemical stress, nutrient levels, and FoxO signaling pathway, and autophagy-related DEGs were involved in the regulation of autophagy, apoptosis, PI3K-Akt signaling, and FoxO signaling pathways. Six candidate genes (*EGFR*, *KRAS*, *IL1B*, *SIRT1*, *ATM*, and *MAPK8*) that contributed to the etiology of myelomeningoceles were selected from the top ten hub genes of ferroptosis- and autophagy-related DEGs using PPI network analyses. Moreover, we explored the TFs and miRNAs that regulate the candidate genes and analyzed the TF-miRNA coregulatory network, as well as diseases and chemicals that interact with the candidate genes. The candidate genes demonstrated high diagnostic value for myelomeningocele. This study serves as a useful reference for elucidating the pathological mechanism of myelomeningocele from the perspective of ferroptosis using bioinformatics analysis.

Ferroptosis is a type of cell death characterized by iron-dependent lipid peroxidation and subsequent membrane damage [5,34]. This process involves the accumulation of reactive oxygen species (ROS) and depletion of glutathione, ultimately leading to cellular dysfunction and death [5]. Previous studies have identified several key components involved in the regulation of ferroptosis, including GPX4, acyl-CoA synthetase long-chain family member 4 (ACSL4), and SLC7A11, which offer potential strategies for preventing or treating ferroptotic cell death [34–36]. Ferroptosis has been implicated in various pathological conditions including neurodegenerative diseases [37], cancer [38,39], and ischemia-reperfusion injury [40]. A growing body research suggests that ferroptosis is

involved in embryonic development. Iron overload in the endometriotic peritoneal fluid causes ferroptosis, which contributes to embryotoxicity [41]. Jiang et al. reported that ferroptosis marker Ptgs2 was significantly upregulated in p53^{3KR/3KR}Mdm2^{-/-} embryo with NTDs phenotype, and that ferroptosis inhibitor ferrostatin-1 can promote the organogenesis including eye formation and limb differentiation [17], indicating the ferroptosis played crucial roles in embryonic development. Qi et al. showed that ferroptosis significantly decreases the axonal length of motor nerves in zebrafish embryos, indicating that activated ferroptosis could impair neurogenesis [8]. However, limited research has been conducted on the relationship between ferroptosis and myelomeningocele. We identified 45 upregulated and 15 downregulated ferroptosis-related DEGs in myelomeningocele compared to control group. The KEGG enrichment analysis demonstrated that ferroptosis-related DEGs were primarily enriched in FoxO signaling pathway. Activating the FoxO signaling pathway promotes ferroptosis to suppress cell viability and metastasis in laryngeal cancer [42]. Based on the above results, ferroptosis-related DEGs may mediate the FoxO signaling pathway, contributing to the occurrence of myelomeningocele.

Autophagy plays a crucial role in maintaining cellular, tissue, and organismal homeostasis by promoting cellular renewal and reducing oxidative stress, and is involved in multiple diseases such as cancer [43], neurodegenerative disorders [44], and NTDs [10]. Autophagy is suppressed in neuroepithelial cells during neural tube development, leading to NTD formation [45]. Ye et al. noted that rare mutations in the autophagy regulator gene *AMBRA1* may contribute to the etiology of human NTDs [11]. We found that 74 autophagy-related DEGs (50 upregulated and 24 downregulated) were associated with the occurrence of myelomeningocele. Autophagy-related DEGs were enriched in the PI3K-Akt and FoxO signaling pathways. Based on the pathway enrichment analysis of ferroptosis- and autophagy-related DEGs, the results demonstrated that the FoxO signaling pathway is involved in these two biological processes, suggesting that this pathway may control the crosstalk between ferroptosis and autophagy. Ferritinophagy is a selective type of autophagy that mediates ferroptosis through the degrading of ferritin [14]. Sun et al. demonstrated that ferritinophagy induces ferroptosis in fetal growth-restricted placentas, indicating that autophagy mediates ferroptosis and is involved in embryonic development [16]. Therefore, ferritinophagy may contribute to the pathogenesis of myelomeningocele.

Five upregulated (*KRAS*, *IL1B*, *SIRT1*, *ATM*, and *MAPK8*) and one downregulated (*EGFR*) candidate genes were selected from ferroptosis- and autophagy-related hub genes using PPI analysis. *SIRT1*, a highly conserved NAD⁺-dependent lysine deacetylase, was required to suppress neurogenesis and induced oligodendrogenesis in neural progenitor cells [46,47]. Activated *SIRT1* deacetylated octamer-binding transcription factor 6 (OCT6) and induced OCT6 ubiquitination/degradation, consequently increasing the incidence of NTDs in mice [48]. However, some inconsistent results have been reported. A microarray study revealed that *Sirt1* was decreased in mouse NTDs induced by valproic acid [49]. Zhao et al. reported that the expression of *Sirt1* was significantly downregulated in all-*trans* retinoic acid-induced rat spina bifida aperta [50]. In the present study, we observed that *SIRT1* expression significantly increased in the amniotic fluid of human myelomeningocele compared to the control group. This is similar to the results of Li et al. [48]. *ATM* is a DNA damage-inducing protein kinase. *ATM* inhibition can decrease histone H2A monoubiquitination, which may be involved in the occurrence of NTDs [51]. A significant increase in *ATM* expression has been observed in human myelomeningocele, further suggesting that *ATM* is involved in the etiology of NTDs. However, little research has been conducted on candidate genes (*KRAS*, *IL1B*, *MAPK8*, and *EGFR*) and NTDs. The underlying mechanism between them needs to be investigated in the future.

To better elucidate the function of the candidate genes in the pathological mechanism of myelomeningocele, TF-gene and gene-miRNA networks were constructed to investigate the regulatory factors of the six candidate genes at the transcriptional and post-transcriptional levels. Here, we observed that TFs such as P53, POU3F2, TATA and E4BP4 are involved in the regulation of candidate genes. P53 a transcription factor involved in the development of NTDs [52,53]. The p53^{N236S} mutation results in decreased neuroepithelial differentiation and apoptosis, increased neuroepithelial proliferation during neurulation, and failure of neural tube closure, leading to the development of NTDs [54]. Li et al. showed that decreased p53 ubiquitination, increased p53 stabilization, and excessive apoptosis contribute to the impairment of neural tube closure [55]. The candidate gene was hypothesized to interact with p53, resulting in the development of myelomeningocele. miRNAs are endogenous noncoding small RNA molecules that target mRNAs to repress translation or trigger mRNA degradation [56–58]. miRNAs play critical roles in neurogenesis and brain development [59, 60]. Altered miRNAs levels are closely associated with the incidence of NTDs [61,62]. In the present study, we observed that miRNAs such as hsa-miR-27a-3p, hsa-miR-877-5p, hsa-miR-892b, hsa-miR-155-5p, hsa-miR-92a-3p, and hsa-miR-18a-3p interacted with candidate genes. Moreover, we showed that miRNAs cooperate with TF to regulate candidate genes. These TFs, miRNAs, and candidate genes may serve as biomarkers for the diagnosis and treatment of myelomeningocele.

Different diseases are associated on the premise that they contain at least one similar gene. In this study, gene-disease analysis was performed to infer the linkage between candidate genes and diseases. The results indicated that the candidate genes for myelomeningocele were associated with diverse diseases, including schizophrenia, fibrosis, and neoplasms. Epidemiological observations suggest that schizophrenia and NTDs shared the similar etiological risk factors such as nutritional deficiencies in utero [63], seasonal variation [64]. Few studies have examined the association between fibrosis, neoplasia, and NTDs. The protein-chemical association network demonstrated that chemicals such as resveratrol, sodium arsenite, cadmium chloride, curcumin, and quercetin interacted with the candidate genes of myelomeningocele. Early maternal exposure to resveratrol could induce NTDs in mice [48]. In contrast to the findings, Zhao et al. showed that resveratrol treatment can decrease the incidence rate of spina bifida aperta induced by all-*trans* retinoic acid in rat embryos [50]. Exposure to sodium arsenite leads to failure in the closure of the caudal end of the neural tube in chicken embryos [65]. Cadmium chloride contributed to the pathogenesis of exencephaly [66]. However, curcumin can reduce high glucose-induced NTDs by blocking cellular stress and caspase activation [67]. Quercetin decreased the incidence of NTDs induced by cyclophosphamide [68]. These studies indicate that sodium arsenite and cadmium chloride contribute to the pathogenesis of myelomeningocele, and resveratrol, curcumin, and quercetin may be promising chemicals for the treatment of NTDs such as myelomeningocele.

This study had some limitations. First, owing to the small sample sizes in the GSE101141 dataset, it was necessary to enlarge the

sample volume to further confirm the association of candidate genes with myelomeningocele. Furthermore, because of the enrichment methods used, there may be false negatives, and other neighboring genes require study. Finally, to better determine the candidate genes as diagnostic and treatment targets, the causal relationship between candidate genes and the pathophysiological mechanisms of myelomeningocele requires *in vivo* and *in vitro* investigation.

5. Conclusions

In our present study, we performed a bioinformatics analysis of ferroptosis- and autophagy-related DEGs, thereby acquiring novel insights into the pathogenesis of myelomeningocele. miRNAs such as hsa-miR-27a-3p, hsa-miR-877-5p, and hsa-miR-892b, and TFs including P53, POU3F2, and TATA are essential for the regulation of candidate genes and contribute to the occurrence of myelomeningocele. Chemicals, such as resveratrol, curcumin, and quercetin may have significant implications in the treatment of myelomeningocele. Candidate genes (*EGFR*, *KRAS*, *IL1B*, *SIRT1*, *ATM*, and *MAPK8*) have high diagnostic value, especially *MAPK8*, which is an interesting target for future in-depth research.

Funding

This research was funded by the Foundation of the Capital Institute of Pediatrics (Grant No. JCYJ-2023-05), and National Natural Science Foundation of China (No. 82201319).

Institutional review board statement

Not applicable.

Informed consent statement

Not applicable.

Data availability statement

The datasets were analyzed from GEO (<https://www.ncbi.nlm.nih.gov/geo>), FerrDb (<http://www.zhouan.org/ferrdb>), and Autophagy Database (<http://hamdb.scbdd.com>). Data supporting the findings of this study are available from the corresponding author upon request.

CRedit authorship contribution statement

Xiuwei Wang: Writing – original draft, Funding acquisition, Formal analysis, Conceptualization. **Kaixin Wei:** Software, Methodology, Formal analysis. **Min Wang:** Writing – review & editing, Validation, Conceptualization. **Li Zhang:** Writing – review & editing, Software, Funding acquisition, Conceptualization.

Declaration of competing interest

The authors declare that they have no known competing financial interests or personal relationships that could have appeared to influence the work reported in this paper.

Acknowledgments

Not applicable.

Appendix A. Supplementary data

Supplementary data to this article can be found online at <https://doi.org/10.1016/j.heliyon.2024.e29654>.

References

- [1] A.A. Alruwaili, M.D.J. Myelomeningocele, StatPearls, Treasure Island (FL) ineligible companies, in: Disclosure: Joe M Das Declares No Relevant Financial Relationships with Ineligible Companies, 2023.
- [2] A.J. Copp, et al., Spina bifida, Nat. Rev. Dis. Prim. 1 (2015) 15007.
- [3] G. Ortiz-Cruz, et al., Myelomeningocele genotype-phenotype correlation findings in cilia, HH, PCP, and WNT signaling pathways, Birth Defects Res 113 (4) (2021) 371–381.
- [4] L. Hebert, et al., Burden of rare deleterious variants in WNT signaling genes among 511 myelomeningocele patients, PLoS One 15 (9) (2020) e0239083.

- [5] X. Jiang, B.R. Stockwell, M. Conrad, Ferroptosis: mechanisms, biology and role in disease, *Nat. Rev. Mol. Cell Biol.* 22 (4) (2021) 266–282.
- [6] H. Qi, et al., Acrolein-inducing ferroptosis contributes to impaired peripheral neurogenesis in zebrafish, *Front. Neurosci.* 16 (2022) 1044213.
- [7] H. Imai, et al., Lipid peroxidation-dependent cell death regulated by GPx4 and ferroptosis, *Curr. Top. Microbiol. Immunol.* 403 (2017) 143–170.
- [8] H. Feng, et al., Transferrin receptor is a specific ferroptosis marker, *Cell Rep.* 30 (10) (2020) 3411–3423 e7.
- [9] R. Song, et al., Sevoflurane diminishes neurogenesis and promotes ferroptosis in embryonic prefrontal cortex via inhibiting nuclear factor-erythroid 2-related factor 2 expression, *Neuroreport* 33 (6) (2022) 252–258.
- [10] G.M. Fimia, et al., Ambra1 regulates autophagy and development of the nervous system, *Nature* 447 (7148) (2007) 1121–1125.
- [11] J. Ye, et al., Rare mutations in the autophagy-regulating gene AMBRA1 contribute to human neural tube defects, *Hum. Mutat.* 41 (8) (2020) 1383–1393.
- [12] F. Wang, et al., Protein kinase C- α suppresses autophagy and induces neural tube defects via miR-129-2 in diabetic pregnancy, *Nat. Commun.* 8 (2017) 15182.
- [13] M. Gao, et al., Ferroptosis is an autophagic cell death process, *Cell Res.* 26 (9) (2016) 1021–1032.
- [14] A. Ajuolabady, et al., Ferritinophagy and ferroptosis in the management of metabolic diseases, *Trends Endocrinol. Metabol.* 32 (7) (2021) 444–462.
- [15] N. Santana-Codina, A. Gikandi, J.D. Mancias, The role of NCOA4-mediated ferritinophagy in ferroptosis, *Adv. Exp. Med. Biol.* 1301 (2021) 41–57.
- [16] Y. Sun, et al., Bisphenol A induces placental ferroptosis and fetal growth restriction via the YAP/TAZ-ferritinophagy axis, *Free Radic. Biol. Med.* 213 (2024) 524–540.
- [17] L. Jiang, et al., Ferroptosis as a p53-mediated activity during tumour suppression, *Nature* 520 (7545) (2015) 57–62.
- [18] T. Tarui, et al., Amniotic fluid transcriptomics reflects novel disease mechanisms in fetuses with myelomeningocele, *Am. J. Obstet. Gynecol.* 217 (5) (2017) 587 e1–e587 e10.
- [19] T. Barrett, et al., NCBI GEO: archive for functional genomics data sets—update, *Nucleic Acids Res.* 41 (Database issue) (2013) D991–D995.
- [20] N.N. Wang, et al., HAMdb: a database of human autophagy modulators with specific pathway and disease information, *J. Cheminf.* 10 (1) (2018) 34.
- [21] G. Zhou, et al., NetworkAnalyst 3.0: a visual analytics platform for comprehensive gene expression profiling and meta-analysis, *Nucleic Acids Res.* 47 (W1) (2019) W234–W241.
- [22] B.T. Sherman, et al., DAVID: a web server for functional enrichment analysis and functional annotation of gene lists (2021 update), *Nucleic Acids Res.* 50 (W1) (2022) W216–W221.
- [23] Y. Liao, et al., WebGestalt 2019: gene set analysis toolkit with revamped UIs and APIs, *Nucleic Acids Res.* 47 (W1) (2019) W199–W205.
- [24] Y. Zhou, et al., Metascape provides a biologist-oriented resource for the analysis of systems-level datasets, *Nat. Commun.* 10 (1) (2019) 1523.
- [25] D. Szklarczyk, et al., STRING v11: protein-protein association networks with increased coverage, supporting functional discovery in genome-wide experimental datasets, *Nucleic Acids Res.* 47 (D1) (2019) D607–D613.
- [26] P. Shannon, et al., Cytoscape: a software environment for integrated models of biomolecular interaction networks, *Genome Res.* 13 (11) (2003) 2498–2504.
- [27] N.T. Doncheva, et al., Cytoscape StringApp: network analysis and visualization of Proteomics data, *J. Proteome Res.* 18 (2) (2019) 623–632.
- [28] H. Dweep, et al., miRWalk—database: prediction of possible miRNA binding sites by “walking” the genes of three genomes, *J. Biomed. Inf.* 44 (5) (2011) 839–847.
- [29] J.A. Castro-Mondragon, et al., Jaspur 2022: the 9th release of the open-access database of transcription factor binding profiles, *Nucleic Acids Res.* 50 (D1) (2022) D165–D173.
- [30] Z.P. Liu, et al., RegNetwork: an integrated database of transcriptional and post-transcriptional regulatory networks in human and mouse, *Database* (2015) 2015.
- [31] J. Pinerò, et al., DisGeNET: a discovery platform for the dynamical exploration of human diseases and their genes, *Database* 2015 (2015) bav028.
- [32] A.P. Davis, et al., Comparative Toxicogenomics database (CTD): update 2023, *Nucleic Acids Res.* 51 (D1) (2023) D1257–D1262.
- [33] N.D. Greene, A.J. Copp, Neural tube defects, *Annu. Rev. Neurosci.* 37 (2014) 221–242.
- [34] D. Liang, A.M. Minikes, X. Jiang, Ferroptosis at the intersection of lipid metabolism and cellular signaling, *Mol. Cell* 82 (12) (2022) 2215–2227.
- [35] Y. Yang, et al., ACSL3 and ACSL4, distinct roles in ferroptosis and cancers, *Cancers* 14 (23) (2022) 5896.
- [36] J.D. Lu, et al., Butylphthalide protects against ischemia-reperfusion injury in rats via reducing neuron ferroptosis and oxidative stress, *J. Invest. Med.* (2023) 10815589231167358.
- [37] Y. Sun, et al., Mechanisms of ferroptosis and emerging links to the pathology of neurodegenerative diseases, *Front. Aging Neurosci.* 14 (2022) 904152.
- [38] L. Zhao, et al., Ferroptosis in cancer and cancer immunotherapy, *Cancer Commun.* 42 (2) (2022) 88–116.
- [39] D. Li, Y. Li, The interaction between ferroptosis and lipid metabolism in cancer, *Signal Transduct. Targeted Ther.* 5 (1) (2020) 108.
- [40] H.F. Yan, et al., The pathological role of ferroptosis in ischemia/reperfusion-related injury, *Zool. Res.* 41 (3) (2020) 220–230.
- [41] S. Li, et al., Iron overload in endometriosis peritoneal fluid induces early embryo ferroptosis mediated by HMOX1, *Cell Death Dis.* 7 (1) (2021) 355.
- [42] M. Xu, et al., Silencing KPNA2 promotes ferroptosis in laryngeal cancer by activating the FoxO signaling pathway, *Biochem. Genet.* (2024), <https://doi.org/10.1007/s10528-023-10655-8>.
- [43] X. Li, S. He, B. Ma, Autophagy and autophagy-related proteins in cancer, *Mol. Cancer* 19 (1) (2020) 12.
- [44] S. Ghavami, et al., Autophagy and apoptosis dysfunction in neurodegenerative disorders, *Prog. Neurobiol.* 112 (2014) 24–49.
- [45] C. Xu, et al., Trehalose prevents neural tube defects by correcting maternal diabetes-suppressed autophagy and neurogenesis, *Am. J. Physiol. Endocrinol. Metab.* 305 (5) (2013) E667–E678.
- [46] T. Prozorovski, et al., Sirt1 contributes critically to the redox-dependent fate of neural progenitors, *Nat. Cell Biol.* 10 (4) (2008) 385–394.
- [47] L.R. Stein, S. Imai, Specific ablation of Nampt in adult neural stem cells recapitulates their functional defects during aging, *EMBO J.* 33 (12) (2014) 1321–1340.
- [48] G. Li, et al., Dysregulation of the SIRT1/OCT6 Axis contributes to environmental stress-induced neural induction defects, *Stem Cell Rep.* 8 (5) (2017) 1270–1286.
- [49] A. Okada, et al., Identification of early-responsive genes correlated to valproic acid-induced neural tube defects in mice, *Birth Defects Res A Clin Mol Teratol* 73 (4) (2005) 229–238.
- [50] L. Zhao, et al., Bhlhe40/Sirt1 axis-regulated mitophagy is implicated in all-trans retinoic acid-induced spina bifida aperta, *Front. Cell Dev. Biol.* 9 (2021) 644346.
- [51] P. Pei, et al., Folate deficiency induced H2A ubiquitination to lead to downregulated expression of genes involved in neural tube defects, *Epigenet. Chromatin* 12 (1) (2019) 69.
- [52] E.R. Lachenauer, et al., p53 disruption increases uracil accumulation in DNA of murine embryonic fibroblasts and leads to folic acid-nonresponsive neural tube defects in mice, *J. Nutr.* 150 (7) (2020) 1705–1712.
- [53] A.R.D. Delbridge, et al., Loss of p53 causes stochastic aberrant X-chromosome inactivation and female-specific neural tube defects, *Cell Rep.* 27 (2) (2019) 442–454 e5.
- [54] J. Zhao, et al., p53 mutant p53(N236S) induces neural tube defects in female embryos, *Int. J. Biol. Sci.* 15 (9) (2019) 2006–2015.
- [55] H. Li, J. Zhang, L. Niswander, Zinc deficiency causes neural tube defects through attenuation of p53 ubiquitylation, *Development* 145 (24) (2018) dev169797.
- [56] D.P. Bartel, MicroRNAs: target recognition and regulatory functions, *Cell* 136 (2) (2009) 215–233.
- [57] W. Filipowicz, S.N. Bhattacharyya, N. Sonenberg, Mechanisms of post-transcriptional regulation by microRNAs: are the answers in sight? *Nat. Rev. Genet.* 9 (2) (2008) 102–114.
- [58] N. Bushati, S.M. Cohen, microRNA functions, *Annu. Rev. Cell Dev. Biol.* 23 (2007) 175–205.
- [59] K.M. Foshay, G.I. Gallicano, miR-17 family miRNAs are expressed during early mammalian development and regulate stem cell differentiation, *Dev. Biol.* 326 (2) (2009) 431–443.
- [60] C. Leucht, et al., MicroRNA-9 directs late organizer activity of the midbrain-hindbrain boundary, *Nat. Neurosci.* 11 (6) (2008) 641–648.
- [61] P. Qin, et al., Altered microRNA expression profiles in a rat model of spina bifida, *Neural Regen Res* 11 (3) (2016) 502–507.
- [62] S. Ramya, et al., Maternal diabetes alters expression of MicroRNAs that regulate genes critical for neural tube development, *Front. Mol. Neurosci.* 10 (2017) 237.
- [63] S. Zammit, et al., Schizophrenia and neural tube defects: comparisons from an epidemiological perspective, *Schizophr. Bull.* 33 (4) (2007) 853–858.

- [64] G. Marzullo, F.C. Fraser, Similar rhythms of seasonal conceptions in neural tube defects and schizophrenia: a hypothesis of oxidant stress and the photoperiod, *Birth Defects Res A Clin Mol Teratol* 73 (1) (2005) 1–5.
- [65] G. Song, et al., Effects of choline on sodium arsenite-induced neural tube defects in chick embryos, *Food Chem. Toxicol.* 50 (12) (2012) 4364–4374.
- [66] B.P. Schmid, J. Kao, E. Goulding, Evidence for reopening of the cranial neural tube in mouse embryos treated with cadmium chloride, *Experientia* 41 (2) (1985) 271–272.
- [67] Y. Wu, et al., Curcumin ameliorates high glucose-induced neural tube defects by suppressing cellular stress and apoptosis, *Am. J. Obstet. Gynecol.* 212 (6) (2015) 802 e1–e8.
- [68] M. Khaksary Mahabady, et al., Protective effect of quercetin on skeletal and neural tube teratogenicity induced by cyclophosphamide in rat fetuses, *Vet. Res. Forum* 7 (2) (2016) 133–138.